Hindawi
Aquaculture Research
Volume 2023, Article ID 1697400, 16 pages
https://doi.org/10.1155/2023/1697400

Research Article

A Cold-Inducible RNA Binding Protein Gene from *Acanthopagrus schlegelii*: Molecular Characterization, Expression, and Association with Apoptosis to Low-Temperature Stress

Wei Mingliang,[1,2] **Shen Mingjun**,[1,2] **Wang Yue**,[1,2] **Gao Bo**,[1] **Sun Ruijian**,[1] **Qin Yali**,[1] **Jiang Jianbin**,[3] **Zhou Jianlou**,[3] **Shen Jing**,[1] **Tang Xiaojian**,[1] **Zhang Zhiyong**,[1] **and Zhang Zhiwei**[1,2]

[1]*Jiangsu Marine Fishery Research Institute, Nantong, China*
[2]*National Demonstration Center for Experimental Fisheries Science Education, Shanghai Ocean University, Shanghai, China*
[3]*Tongzhou Aquatic Technology Promotion Station, Nantong, China*

Correspondence should be addressed to Zhang Zhiwei; zhzhwei2005@126.com

Received 5 December 2022; Revised 26 May 2023; Accepted 7 June 2023; Published 20 June 2023

Academic Editor: Pravesh Kumar

In this study, the complete cDNA sequence (1552 bp) of the cold-inducible RNA binding protein gene (*cirbp* gene) was successfully cloned from the liver in *Acanthopagrus schlegelii* (initial weight: 15.0 ± 2.3 g). Results showed that *Ascirbp* (*cirbp* gene from *A. schlegelii*) gene has 24 phosphorylation sites, no signal peptide, and no transmembrane helix structure. AsCIRBP, with a molecular weight of 18.84 ku and an isoelectric point of 9.04 was a stable protein that encodes 182 amino acids. Subcellular localization analysis of this protein showed that it was located in the nucleus. Sequence alignment results showed that the AsCIRBP amino acid sequences of various fishes including black porgy were highly conserved, especially the RNA recognition motif (RRM). Those results of real-time quantitative PCR (qRT-PCR) demonstrated that *Ascirbp* gene was specifically expressed in the liver tissue of black porgy and its expression was significantly increased under cold stress or cold acclimation. The RNA interference experiment results showed that *Ascirbp*-dsRNA could suppress the expression of *Ascirbp* gene in the liver of black porgy through intraperitoneal injection. After silencing the expression of *Ascirbp* gene, RNAi groups were more severely damaged in the structure of the liver tissue and more prone to apoptosis under cold stress than control groups. The results of the study on the linkage between *Ascirbp* gene expression and mitochondrial apoptosis pathways showed that changes in the expression of the *Ascirbp* gene had a significant effect on the expression of key genes of apoptosis. The most striking result from silencing the expression of the *Ascirbp* gene was that expressions of the *bcl*-2 and *apaf*-1 gene in the liver of black porgy decreased significantly, which can block the normal apoptotic process. After the disruption of the normal apoptotic process, the expressions of *p*53, *bax*, *cyto-c*, *caspase*-9, *caspase*-3, *diablo*, and *caspase*-1 gene were significantly affected. These results suggest that *Ascirbp* gene can inhibit apoptosis and protect tissue structure in the liver tissue of black porgy at low temperatures.

1. Introduction

Black porgy (*Acanthopagrus schlegelii*) belongs to the family Sparidae in the order *Perciformes* [1], which is widely distributed along the western Pacific coast because of its wide temperature and salinity tolerance. It is an essential coastal economic fish in China, Japan, and Southeast Asia [2]. The suitable growth water temperature of black porgy is ranged from 15 to 25°C [3]. When the environmental water temperature decreased to 5°C, black porgy cannot survive for a long time [4]. So, the fish cannot be naturally overwintering outdoors when farmed in the northern part of China. This problem has hindered the promotion of the black porgy artificial culture in coastal China for a long time. Farmers usually adopt some traditional overwintering methods to improve survival rate, such as bringing them indoors or increasing the aquaculture water temperature [5]. However, these methods will increase the cost of breeding

black porgy and limit the promotion of this fish. Therefore, cultivating low-temperature tolerance varieties of black porgy plays a great role in promoting the sustainable development of its aquaculture industry.

When the fish is in a low-temperature environment, they will resist and repair the damage caused from low temperatures by adjusting physiological changes [6]. When it exceeds the physiological tolerance range of the body, apoptosis will occur [7]. Apoptosis is autonomously regulated by organisms to adapt to the environment [8]. Previous studies have shown that the body will remove these useless and damaged cells through apoptosis when cells of multicellular organisms undergo natural aging or are damaged by external factors [8]. For example, during the development of a vertebrate embryo, the organism removes cells that form unwanted structures by means of apoptosis [9, 10]. Cold-inducible RNA binding protein (CIRBP) is a kind of protein induced by cold stress that responds to regulation associated with apoptosis [11]. Previous studies have shown that the overexpression of CIRBP can inhibit apoptosis [12–14]. Therefore, the research about CIRBP inhibiting apoptosis is gradually attracting attention. Some studies have concluded that CIRBP is mainly presented in stress granules in the nucleus under no external stimulation [15]. When living organism subjected to environmental stress, their cells would initiate the apoptotic pathway [11]. CIRBP translocates from the nucleus of the cell to the cytoplasm and inhibits apoptosis [16]. CIRBP can specifically inhibit the mitochondrial apoptosis pathway in damaged cells [17]. This pathway is accurate one in the research of apoptosis pathway at present. The mitochondrial apoptotic pathway, which is intrinsic to apoptosis, is triggered by the release of cytochrome c (*cyto-c*) from mitochondria [18]. In the apoptosis pathway, some genes play extremely important roles. Nine capital genes of them are the apoptotic protease activating factor-1 gene (*apaf-1* gene), *bcl*-associated gene (*bax* gene), b-cell lymphoma-2 gene (*bcl*-2 gene), cysteinyl aspartate specific proteinase-1 gene (*caspase*-1 gene), cysteinyl aspartate specific proteinase-3 gene (*caspase*-3 gene), cysteinyl aspartate specific proteinase-9 gene (*caspase*-9 gene), cytochrome c gene (*cyto-c* gene), direct IAP binding protein with low pI gene (*diablo* gene), and the *p*53 tumor suppressor gene (*p*53 gene). Related research shows that CIRBP can significantly affect the expression of the Bcl-2 protein [19]. CIRBP can affect Bcl-2 protein by regulating *p53* protein [20]. Bcl-2 protein can regulate the permeability of the mitochondrial membrane together with *bax* protein and release the Cyto-*c* in the mitochondria into the cytoplasm [21]. Cyto-c can bind to Apaf-1 protein, and the combination will promote the express of Caspase-9 protein to activate Caspase protein for apoptosis [22]. Diablo protein can bind to the interlocking family of apoptosis-inhibiting proteins [23]. Then, Diablo protein activates Caspase-3 protein to execute the apoptotic program [23]. The *caspase*-1 gene can mediate the inflammatory response and activates pyroptosis [24]. The function of these apoptotic genes is being revealed, and the purpose of this experiment is also to study the interaction between CIRBP and apoptosis.

In related studies, researchers have obtained the sequences of the *cirbp* genes of bastard halibut (*Paralichthys olivaceus*) [25], yellow drum (*Nibea albiflora*) [26], obscure puffer (*Takifugu obscurus*) [27], large yellow croaker (*Larimichthys crocea*) [28], and other fish. The *cirbp* gene is involved in the stress mechanism of these fishes under low temperatures, osmotic pressure, and other stresses. However, it is still unclear whether *Ascirbp* gene plays a role in black porgy. The aim of this study was to investigate the function of *Ascirbp* gene by RNAi technique and explore whether the gene was involved in the regulation of apoptotic pathways. It is hoped that this research will contribute to a deeper understanding of the mechanisms of black porgy responds to low-temperature stress and provide some new ideas on exploring the gene function of black porgy.

2. Materials and Methods

2.1. Animals. This study was approved by the Marine Fisheries Research Institute of Jiangsu Province (China). All experiments were carried out following the Guideline for the Care and Use of Experimental Animals of China. All animals used for experiments comply with the Code of Ethics for Animals. The black porgy (initial average weight of 15.0 ± 2.3 g) in this study were taken from the Marine Fisheries Germplasm Innovation Center of Jiangsu Province (Nantong, China). Prior to the experiment, fish were acclimated for two weeks in a concrete pool containing aerated seawater (28% salinity, pH = 8.0, $15.0 \pm 0.5^{\circ}$C). During the acclimatization period, fish were fed twice a day with commercial pelleted feed with a protein content is 48%.

2.2. Experimental Design. To identify the potential roles of *cirbp* in *A. schlegelii*, the following three steps were carried out: (1) cloning and characterization of *Ascirbp* gene, (2) examining the relative expression of *Ascirbp* gene in various tissues, (3) assessing the changes in structural damage of tissue, apoptosis, and expression of apoptosis-related genes in fish at low temperature after silencing expression of *Ascirbp* gene. Three individuals were used to clone *Ascirbp* gene and three fish were used to detect the relative expression of *Ascirbp* gene in various tissues. 60 individuals were used to detect the effect of silencing the expression of *Ascirbp* gene. 1800 individuals were used for the cold stress and cold acclimation experiments, and 180 individuals were used for the RNA interference experiments. In the calculation, 2046 individuals were used in the present research.

2.3. Cloning and Characterization of Ascirbp Gene

2.3.1. Sampling. Three individuals were used for this study and were randomly selected for sampling in the black porgy temporarily raised at 15°C. Before sampling, black porgy were lightly anesthetized with tricaine methane sulfonate (MS-222, USA). Liver, gill, muscle, heart, kidney, brain, and other tissue samples obtained from black porgy were frozen in liquid nitrogen and stored at −80°C for gene cloning. Total

RNA was extracted from the liver of black porgy using the Spin Column Animal Total RNA Purification Kit (Sangon Biotech, China) according to the manufacturer's protocol. The concentration of total RNA was measured with a Nanodrop 2000 nucleic acid analyzer (Thermo, USA). The quantity and quality of RNA were examined by UV-spectrophotometry (OD260/OD280) and agarose gel electrophoresis, respectively. Total RNA from liver was reversed into first-strand cDNA using the M-MuLV First Strand cDNA Synthesis Kit (Sangon Biotech, China) according to the manufacturer's instructions.

2.3.2. Cold Stress and Cold Acclimation. Before the low-temperature challenge experiment, black porgy was acclimatized into a separate cement pond with aerated seawater for 24 h. 1800 individuals were randomly divided into six cement ponds (length × width × height: 3.9 m × 2.6 m × 0.9 m), with 300 individuals per cement pond and an air pump for aeration. Two cold circulation systems (Nantong, China) were used to control the water temperature. In one cold circulation system, the water temperature of three cement ponds (cold stress group) decreased from 15°C to 5°C at the rate of 1°C/h, three individuals were randomly collected after maintaining for 0 h, 6 h, 12 h, 18 h, and 24 h at each temperature point of 15°C, 10°C, and 5°C. In the other cold circulation systems, the water temperature of three cement ponds (cold acclimation group) was decreased from 15°C to 5°C at the rate of 1°C/d. Then, three individuals were randomly collected after maintaining for 1 d, 2 d, 3 d, 4 d, and 5 d at each temperature point of 15°C, 10°C, and 5°C. Before sampling, black porgy were randomly collected and lightly anesthetized with tricaine methane sulfonate (MS-222, USA). Liver, gill, muscle, heart, kidney, brain, and other tissue samples obtained from black porgy were frozen in liquid nitrogen and stored at −80°C for the next steps.

2.3.3. PCR and Subcloning of Ascirbp cDNA. The cDNA sequence of the *Ascirbp* gene was obtained from the liver by a reverse-transcription polymerase chain reaction (RT-PCR) and by 3′ and 5′ rapid amplification of cDNA ends (RACE) methods. The cDNA sequence of *Ascirbp* gene was extended by using the SMARTer™ RACE cDNA Amplification Kit (Clontech, USA) according to the manufacturer's protocol. The specific primers for *Ascirbp* gene (Table 1) were designed according to the whole genes of black porgy obtained by the group in the previous study [29]. The initial RT-PCR was performed using degenerate primers (Table 1: *Ascirbp*-F1 and *Ascirbp*-R1). PCR amplification was carried out using Ex Taq polymerase (Takara, Japan) under the following cycling conditions: an initial denaturation step (94°C, 2 min), followed by 35 cycles of denaturation (95°C, 30 s) annealing (55°C, 30 s), and extension (72°C, 1 min), ending with a 10-minute extension phase at 72°C. The target PCR products were purified using the Mag-MK Gel DNA Purification Kit (Sangon Biotech, China) and then cloned into the vector. After that, sequence analysis was conducted on the selected positive clones. Specific primers (Table 1: *Ascirbp*- 3′gsp and *Ascirbp*- 5′gsp) were designed according to the partial fragment of *Ascirbp* gene obtained by cloning. 3′-Full RACECore Set Ver.2.0 (Takara, Japan) and BD SMART TM RACE cDNA Amplification Kit (Clontech, USA) were used for 3′ RACE and 5′ RACE to amplify the 3′ and 5′ end sequences of *Ascirbp* gene cDNA sequences, and the steps and operations were performed according to the instructions. The synthesis and sequencing of primers was performed by Sangon Biotech (Shanghai, China).

2.3.4. Sequence Analysis of Ascirbp Gene and Phylogenetic Analysis. The vector sequences were removed from the sequencing results using SeqMan software and then spliced. The open reading frame (ORF) and amino acid sequences of cDNA sequences were predicted using EditSeq software. *Ascirbp* gene was analyzed and compared using the BLASTX and BLASTP search programs (https://blast.genome.ad.jp) with a GenBank database search. The ORF Finder (https://www.ncbi.nlm.nih.gov/gorf/gorf.html) was used to find the open reading frames of the spliced cDNA sequences. The Expert protein analysis system (https://www.expasy.org/) predicted the corresponding protein molecular weight and isoelectric point. The online SWISS-MODEL software (https://swissmodel.expasy.org/interactive) predicted the three-dimensional structure of protein three-dimensional structure. The SignalP 5.0 Server (https://www.cbs.dtu.dk/services/SignalP/) was used to predict its signal peptide and the molecular mass of mature AsCIRBP was estimated by DNAMAN 8. N-glycosylation sites were predicted via the NetNGlyc 1.0 Server (https://www.cbs.dtu.dk/services/NetNGlyc/).

A phylogenetic tree was constructed for CIRBP based on the neighbor-joining (NJ) method using MEGA-X software [27]. The following protein sequences were used for alignment: CIRBP of zebrafish (*Danio rerio*; AAH48027), tropical clawed frog (*Xenopus tropicalis*; CAJ83306), copperband butterflyfish (*Chelmon rostratus*; XP_041805554), *Anoplopoma fimbria* (*Anoplopoma fimbria*; ACQ58801), Atlantic salmon (*Salmo salar*; NP_001133148.1), elephant shark (*Callorhinchus milii*; NP_001279973), yellowfin seabream (*Acanthopagrus latus*; XP_036939356), American alligator (*Alligator mississippiensis*; NP_001274230), rainbow trout (*Oncorhynchus mykiss*; NP_100305215), mouse (*Mus musculus*; NP_031731), and human (*Homo sapiens*; NP_001271).

2.3.5. Tissue-Specific Ascirbp Gene Expression Analysis. Three individuals were used for this study and randomly selected to sample in the black porgy temporarily raised at 15°C. The sampled fish were lightly anesthetized and sacrificed to obtain various tissues, including the liver, brain, muscle, gills, kidney, heart, and intestine. The above tissue samples and tissue samples (Step 2.3.2) obtained after low-temperature treatment were prepared to elucidate the expression of *Ascirbp* gene by real-time quantitative PCR (qRT-PCR) analyses, while *β-actin* was used as internal reference gene. Sequences of the specific primers for *Ascirbp* gene (*Ascirbp*-qF and *Ascirbp*-qR) were shown in Table 1.

For the qRT-PCR analysis, *Ascirbp* expression levels of three fish were individually determined using the ABI

Table 1: Primer information.

Primer	Primer sequences (5′-3′)	Function	Efficiency of qPCR (%)
Ascirbp-F	AGGGCTGAGTTTCGAGACCA	cDNA validate	—
Ascirbp-R	GCTTACCATAGCCGTCATATCCG		
Ascirbp-3′gsp1	CTCGCTGTATCCACCCTGACCCCTA	3′RACE	—
Ascirbp-3′gsp2	TCACCTCCGAAGCCCCTATCGCCGTA		
Ascirbp-5′gsp1	CGCTTCGGCATACGGAACCATCGAAA	5′RACE	—
Ascirbp-5′gsp2	ACGCTAAAGACGCCATGAACGCAAT		
dsAscirbp-F	GGCTATGCTGCACACGAGTA	RNAi	—
dsAscirbp-R	TGGACAGTAAGTCGACAGCG		
ds (T7) Ascirbp-F	TAATACGACTCACTATAGGGGGCTATGCTGCACACGAGTA		—
ds (T7) Ascirbp-R	TAATACGACTCACTATAGGGTGGACAGTAAGTCGACAGCG		
Ascirbp-qF	GCAATGAACGGCAAGTCTC	qPCR	92.6
Ascirbp-qR	TAACTCCTGTCACCATAACTCC		
β-actin-qF	CGACGGTCAGGTCATCAC		91.9
β-actin-qR	GCCAGCAGACTCCATTCC		
apaf-1-qF	AGACTACGAAGCTGCACACGTCCT		95.0
apaf-1-qR	ATCCCGTCCTGCCATCACGTACC		
bax-qF	AAGGCGCTGACCACCAACC		91.0
bax-qR	GGCTACTGTCCTCCACCGAGA		
bcl-2-qF	ACCATCGTCACCTCCGACTCC		103.7
bcl-2-qR	ACTTTGGGCGAGTTCTTTGTCGT		
caspase-1-qF	GAGACAGCCCGATCCACTCCCAC		97.4
caspase-1-qR	AGCAGAGACCCTTTGACCGAGTGT		
caspase-3-qF	ATGGACTACCCCAGCCTCGGAAC		106.2
caspase-3-qR	GCAGCATCAACATCCGTCCCGTT		
caspase-9-qF	ACTCATACACAGACGCCAAC		94.8
caspase-9-qR	ATGTACTTCTTGGGGTTCTC		
cyto-c-qF	CGGACACTGCCTGATCATAA		96.3
cyto-c-qR	TGCTCTCCAGTTTGTCACAG		
diablo-qF	CAATGCTGTCAACCTGTG		94.2
diablo-qR	TCTTATCTGCGTCTGCTG		
p53-qF	ACGACCATCCTGCTGAGCTT		97.7
p53-qR	ACCTCCGGCCCAAAACAAGT		

7300plus Real-Time PCR system (Applied Biosystems, USA) with SuperReal PreMix Plus kit (TIANGEN, China). The qRT-PCR was carried out in a total volume of 20 μL containing 10 μL of 2 × SuperReal PreMix Plus, 0.6 μL of forward primers (10 μM), 0.6 μL of reverse primers (10 μM), 1 μL of the cDNA template, 2 μL of 50 × ROX Reference Dye, and 5.8 μL of diethylpyrocarbonate (DEPC)-H_2O. The program settings for qRT-PCR were 95°C for 10 min followed by 40 cycles of 95°C for 15 s, 60°C for 30 s, and 72°C for 31 s. Each cDNA sample of each fish was run individually and in duplicate. After the program had finished running, we obtained the cycle threshold (CT) and the relative expression of the tested genes from the ABI software.

2.4. RNA Interference (RNAi)

2.4.1. dsRNA Treatment. The program of RNA interference was designed from reference [30]. The template for the synthesis of *Ascirbp*-dsRNA was prepared by the liver cDNA of black porgy with the primers (*d s*(T7) *Ascirbp*-F and *ds*(T7) *Ascirbp*-R; the underlined part was the T7 promoter; Table 1); dsRNA were synthesized for *Ascirbp* in vitro by using the T7 RNAi Transcription Kit (Vazyme, China) according to the manufacturer's instructions. Primers (Table 1) were designed based on the cDNA sequence of *Ascirbp* gene to produce an amplicon of 388 bp. We measured the concentration of dsRNA at 260 nm with a Nanodrop 2000 nucleic acid analyzer (Thermo, USA). We examined the purity and integrity of dsRNA by electrophoresis of 1.5% agarose gel and then stored it at −20°C until used.

2.4.2. Injection of Ascirbp-dsRNA and Cold Stress Experiments. A preliminary experiment showed that the optimal interference effect was observed after intraperitoneal injection of *Ascirbp*-dsRNA at a dose of 5 μg/g, to investigate the effect of *Ascirbp*-dsRNA to silence the expression of *Ascirbp* gene. We divided black porgy (initial weight: 15.0 ± 2.3 g) randomly into eight groups with 30 fish per group. Four groups were injected with *Ascirbp*-dsRNA at a dose of 5 μg/g, and the remaining four groups were injected with physiological saline. The group injected with *Ascirbp*-dsRNA was named the RNAi group, and the group injected with physiological saline was named the control group. We obtained liver samples at 1 h, 12 h, 24 h, 36 h, and 48 h after injection at 15°C, and obtained three fish samples per group (one RNAi group and one control group) every time.

Based on the results of the preexperiment, repeat injections were performed two days after the injection. After

24 h of repeated injections, the fish were subjected to cold stress experiments. In one cold circulation system, the water temperature of six groups (three RNAi groups and three control groups; 30 fish in per group) decreased from 15°C to 5°C at a rate of 1°C/h. Six individual livers per group were randomly collected after maintaining for 24 h at 15°C, 10°C, and 5°C. Three livers were snap frozed in liquid nitrogen and conserved them at −80°C for gene expression analysis. Furthermore, three samples were excised and fixed in PFA (phosphate buffered saline: formaldehyde = 9 : 1) at room temperature overnight.

2.4.3. H.E. Staining and TUNEL Staining. The paraformaldehyde-fixed livers were rinsed with running water and treated with 70~95% ethanol for dehydration in sequence. After the fixed tissue samples were sectioned and H.E staining, the sections were observed under the microscope for pathological structure. After paraffin tissue sections of black porgy liver were stained with TUNEL according to the instructions of the Biotin TUNEL apoptosis kit (BOSCIENCE, China), observed under a microscope, and photographed for recording.

2.4.4. qRT-RCR. The relative expression of *Ascirbp*, *apaf*-1, *bax*, *bcl*-2, *caspase-1*, *caspase*-3, *caspase*-9, *diablo*, *cyto-c*, and *p*53 genes were tested by qRT-RCR, primers used as shown in Table 1. Primers for *apaf*-1, *bax*, *bcl*-2, *caspase*-1, *caspase*-3, and *diablo* genes referenced from previous studies [5]. The procedure of this experiment refers to Step 2.3.5.

2.5. Data Statistics and Analysis. The $2^{-\Delta\Delta Ct}$ method was used to calculate the relative expression of target genes after real-time fluorescence quantitative PCR analysis. The image data was processed using Adobe Illustrator software. Data obtained from each experiment were expressed as mean ± standard deviation, and the data were processed and analyzed using an ANOVA test between groups at different temperatures at the same time and within groups at different times at the same temperature, and all experimental data were statistically analyzed, as well as plotted using Origin software.

3. Results

3.1. Cloning and Sequence Analysis of Ascirbp Gene. By RT-PCR and RACE methods, the cDNA sequence of *cirbp* gene was obtained from the liver of *A. schlegelii* and named it *Ascirbp* gene. The sequence was deposited in GenBank and the accession number of the gene was obtained as ON063224. As shown in Figure 1, the cDNA sequence of *Ascirbp* gene was 1552 bp in length, which contained a 549 bp open reading frame (ORF), a 71 bp 5′-untranslated region (UTR), a 932 bp 3′-UTR, a stop codon (taa), and a poly A tail.

3.2. Physicochemical Properties and 3D Structure Analysis of AsCIRBP. The physical and chemical properties of AsCIRBP were analyzed by ProtParam, and results showed that the protein was composed of 182 amino acids, with an estimated molecular mass of 18.84 kDa, and a theoretical pI of 9.04. The formula of AsCIRBP was $C_{793}H_{1204}N_{260}O_{273}S_3$, having 2533 atoms in total, 25 negatively charged residues (Asp + Glu), and 28 positively charged residues (Arg + Lys). The instability index was 35.70. Therefore, this protein was classified to be stable according to the criterion that assigns a protein with instability coefficient <40 as stable, and >40 as unstable. The results of the ProtParam analysis showed that the aliphatic index of AsCIRBP was 30.11. The highest score (1.400) was found at Arg11 which was the most hydrophobic site; the lowest score (−2.922) was at aspartic Cys42, which was the most hydrophilic site. Most of the amino acids showed negative values, so it is presumed that AsCIRBP is a hydrophilic protein. The signal peptide of AsCIRBP was predicted with Signal P5.0, a signal peptide prediction server that AsCIRBP had no signal peptide. The TMHMM prediction showed that there were no transmembrane regions.

The subcellular localization analysis of the Protcomp 9.0 protein showed that AsCIRBP was most likely to be located in the nucleus with a value of 4.67, followed by the cytoplasm with a value of 0.27. Using Net NGlyc 1.0 Server and NetOGlyc 4.0 Server to analyze the glycosylation sites. It revealed that AsCIRBP had no N-glycosylation sites and 7 O-glycosylation sites (amino acid residues 87, 102, 104, 132, 147, 165, and 168). Using NetPhos 3.1 Server to analyze the phosphorylation sites, AsCIRBP had 24 phosphorylation sites, including 15 serines (amino acid residues 2, 13, 20, 45, 87, 102, 104, 115, 120, 132, 147, 148, 165, 168, and 170 amino acid residues), 2 threonines (amino acid residues 16 and 42), and 7 tyrosines (amino acid residues 53, 121, 146, 155, 171, 175, and 178).

The secondary structure of AsCIRBP was predicted through the website Prabi. The results showed that the main type of secondary structure of this protein was a random coil. The random coil accounted for 51.65%, the alpha helix accounted for 12.09%, beta-turn accounted for 17.58% and extended strand accounted for 18.68%. The tertiary structure of AsCIRBP was analyzed by the homologous modeling method based on the SWISS-MODEL website. The overall structure of the protein was dominated by random coils, followed by extended strands, and less by alpha-helix. 3D structural modeling of black porgy, human, zebrafish and mouse showed that the structure of AsCIRBP was similar to that of CIRBP from human, zebrafish, and mouse (Figure 2). The score of QMEAN for AsCIRBP was 0.41.

3.3. Sequence Alignment Analysis of AsCIRBP. Sequence alignment showed that the amino acid sequences of CIRBP in various fishes including black porgy were highly conserved, especially the N-terminal RNA recognition motif (RRM) was highly conserved (Figure 3). The constructed phylogenetic tree showed that the CIRBP sequences of bony fishes clustered into one large branch with a sequence similarity of 48.25%–79.39%. Among them, marine fishes such as black porgy, yellowfin seabream, *Anoplopoma fimbria*, and copperband butterflyfish clustered into one small branch before clustering with freshwater fishes such as

```
   1 ACATGGGGATTCGCTCTGCAGCTCCGCTCCTCTTCTGGTCGATACCTCTCGGAGGGAAAGCTACACTAAAGatgtcggacgagggtaaactgtttatcggagggctgagtttcgagacca 120
   1                                                                 M  S  D  E  G  K  L  F  I  G  G  L  S  F  E  T   16
 121 acgaggagtctctggctgcggccttcggcaaatacggaaccatcgaaaaagtggatgtgatcagagacaaagagacggggagatctcgcgggttcggcttcgtgaaatacgacaatgcag 240
  17 N  E  E  S  L  A  A  A  F  G  K  Y  G  T  I  E  K  V  D  V  I  R  D  K  E  T  G  R  S  R  G  F  G  F  V  K  Y  D  N  A   56
 241 atgacgctaaagacgccatgaacgcaatgaacggcaagtctctagatggccgggctattcgcgtggatgaggcaggaaagggtggtcgttccagaggaggtttccaggcaggtggacgcg 360
  57 D  D  A  K  D  A  M  N  A  M  N  G  K  S  L  D  G  R  A  I  R  V  D  E  A  G  K  G  G  R  S  R  G  G  F  Q  A  G  G  R   96
 361 gaggtggaagattcagtggatcaaggggggcgaggtggttacaacggtgacaggagttatggtgacaggagttacggcgatagggggcttcggaggtgagggcaggagctttggaggtggcg 480
  97 G  G  G  R  F  S  G  S  R  G  R  G  G  Y  N  G  D  R  S  Y  G  D  R  S  Y  G  D  R  G  F  G  G  E  G  R  S  F  G  G  G  136
 481 gcggcggtggatacaggagtggaggatattcctcaggaggtggcggcggcggctacagagacaataggggtcagggtggatacagtgagcgctctggatcataccgtgacggatatgacg 600
 137 G  G  G  G  Y  R  S  G  G  Y  S  S  G  G  G  G  G  G  Y  R  D  N  R  G  Q  G  G  Y  S  E  R  S  G  S  Y  R  D  G  Y  D   176
 601 gctatgctgcacacgagtaaACATCTCCCTGATTCAAGATCATCACTTGGCTGGCTGTATTTCAAAGATGCGCTCCTCAAGAAAAATGTCCACGTGTTATTGCTGACCTTAGTTTTGTAG 720
 177 G  Y  A  A  H  E  *                                                                                                  182
 721 TTCTGTTGTAGTAGCTCAAGCATCTTAAAAAAAAAAAATGTAGCCATGAGTTTTGGTCATTCCTTTAACAAACCCATGTTACAAATTACAGTTCAAGACTCTTGCCTTGCTCAATTGGGCA 840
 841 TCTTGATTCCTCAAAGATCGTTTGTTAACTAAAGGCATCTGTATAATCTGATTATTACTCAAGTCCCAATCTGGGGATCAAACAACGGCTCTCCACATGGCTTTTCGTTGAACGGCCACT 960
 961 ACCATCGCTGTCGACTTACTGTCCAGCACGTTAAAGTGTTTCCTGATTTTTGATTCCTTTTTTTGTTAGTTTTTGTTTATTTTTATACTGATATCCGATGGGGCTTGTTTTTTGTTTTTT 1080
1081 CCTTATTTCCCCTTCAGTCTTCGACTGACCTACCTCTTGCCAGGTTTTAAACTGAGTGAGGAAAGGGAGCTTATTAATAGGCTTTTGGGGATTTGTGCTAAATTCCTTTTTACTATTAAA 1200
1201 AACTTAGTTTAGCTGAGGCTCCTGTGTGTTCAATTTCCCAAAAGAGTGAATTCCTTTCAGACTGGTGAACTCCCCCTCCGAAGTGGCCGGCTGTTCATGAAGTCTGTCCAAGGTATTTGC 1320
1321 TGTGCTCTGCTCAACATCTGCATTTTAAATGTGCTGTAAAATGGACTAATCTTGTTTAAGTGATCGAAAAAAAATGTAACTTCGTTTCCCCAAAGTAAAATCTCACCCGGGAACAGTTTTG 1440
1441 TACTTTATGTTCTTTGTATGATCAACATTTTTTTTTTTTTTGTCAGTTTGGCTTCATGGAGCCTATTAAACAGACTGTGCAAAAAAAAAAAAAAAAAAAAAAAAAAAAAAAGT          1552
```

Figure 1: The cDNA sequence of *Ascirbp* gene. CDS was shown in small letters, while 5′UTR and 3′UTR were shown in capital letters. The deduced amino acid sequence was shown by a single-letter code of amino acids below the CDS. "*" represents the conserved sequence of the stop codon, and the RRM superfamily (5-84aa) was underlined.

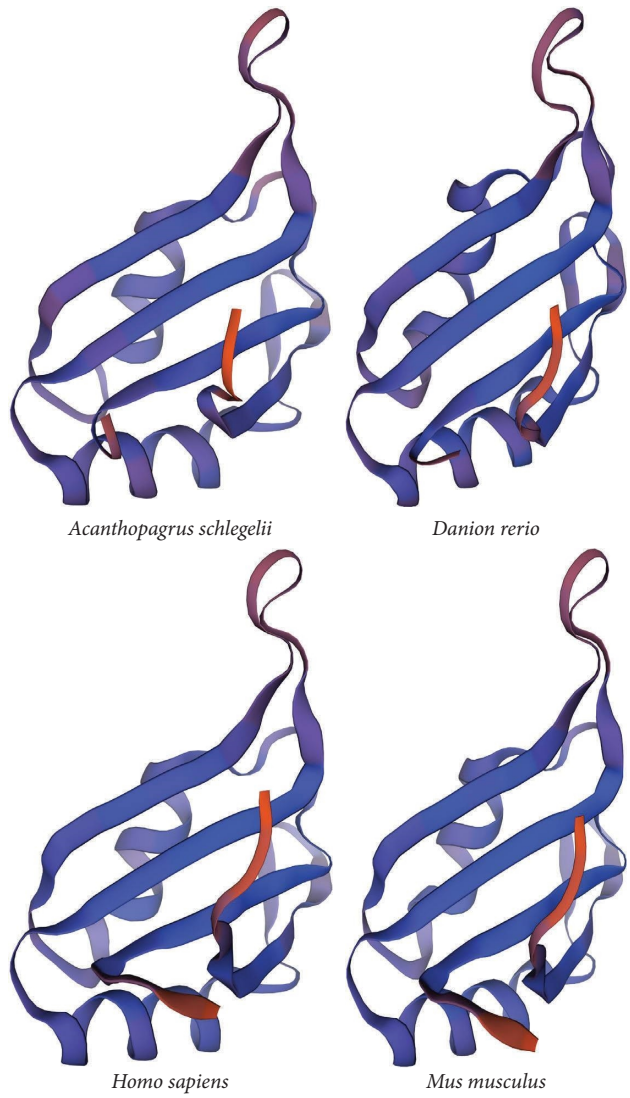

Figure 2: 3D structure model diagram based on SWISS-MODEL prediction of CIRBP among different species.

rainbow trout and zebrafish. Among bony fish, the amino acid sequence of CIRBP in black porgy had the highest similarity (79.39%) with that of yellowfin seabream and the least similar to that of rainbow trout (48.25%). The sequences of CIRBP in bony fishes were less than 45% similar to those of mammals, reptiles, amphibians, and cartilaginous

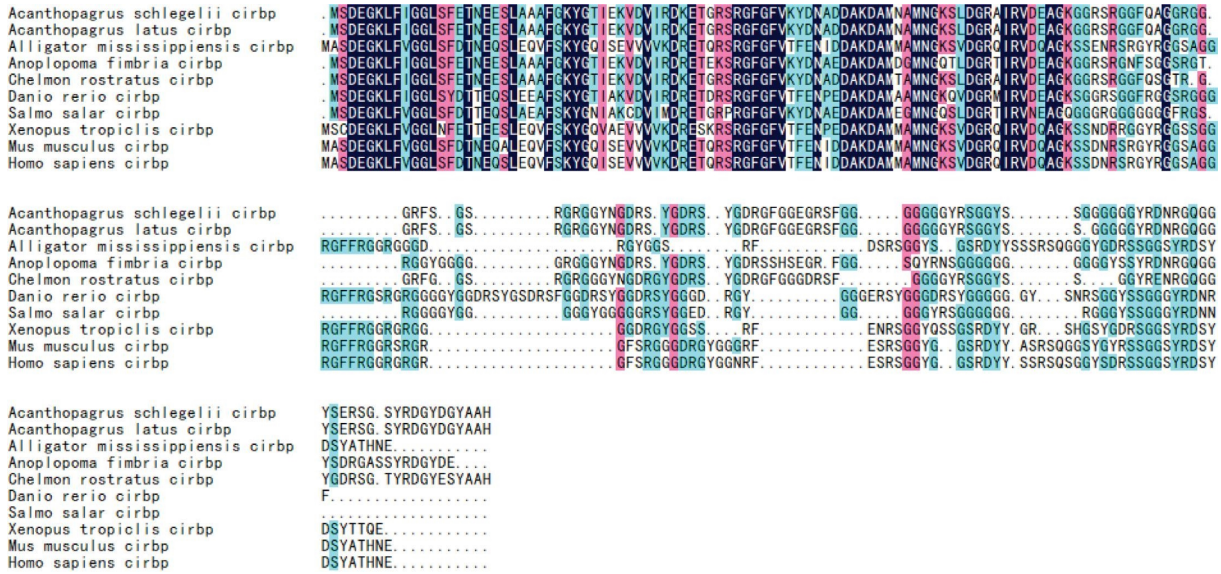

Figure 3: Alignment of multiple sequences of AsCIRBP with other species: yellowfin seabream (*A. latus*), *Anoplopoma fimbria* (*A. fimbria*), American alligator (*A. mississippiensis*), copperband butterflyfish (*C. rostratus*), zebrafish (*D. rerio*), Atlantic salmon (*S. salar*), tropical clawed frog (*X. tropicalis*), mouse (*M. musculus*), and human (*H. sapiens*). Missing amino acids are marked by dots (.).

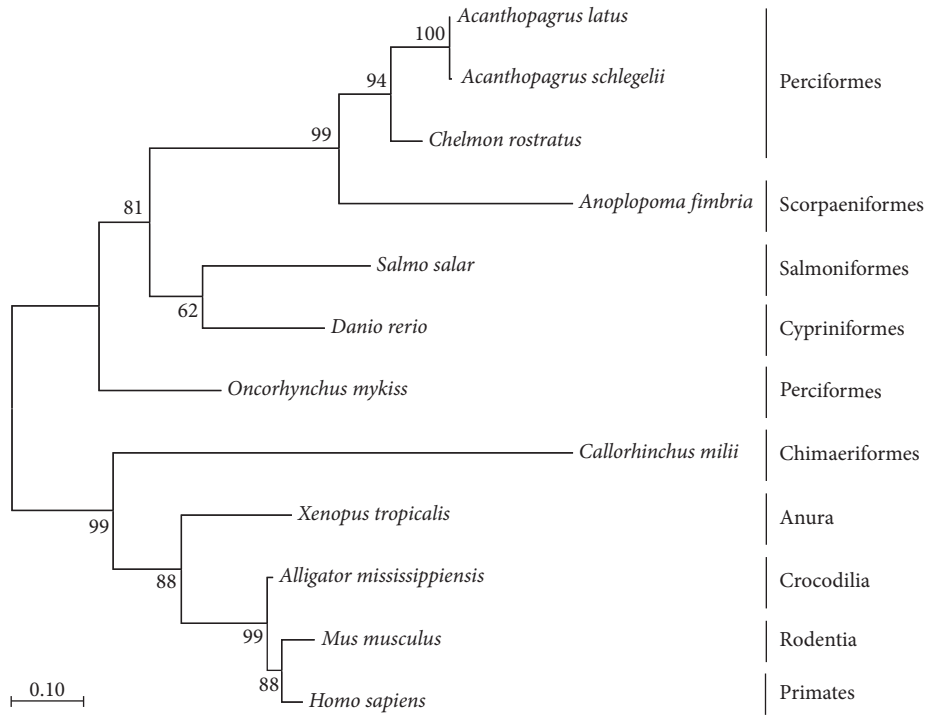

Figure 4: The phylogenetic tree based on amino sequence alignment for CIRBPs in vertebrates.

fishes, which were far apart in the phylogenetic tree (Figure 4).

3.4. Expression Pattern of Ascirbp Gene. Under normal growth water temperature (15°C), the expression of *Ascirbp* gene was the highest in the liver of black porgy ($P < 0.05$, Figure 5(a)). *Ascirbp* gene was expressed in the kidney, intestine, and brain, and weakly expressed in all other tissues ($P < 0.05$, Figure 5(a)).

Ascirbp gene of the liver under cold stress (Figures 5(a) and 5(b)) and cold acclimation (Figure 5(b)) were in the presence of different regulatory patterns. 15°C was used as the control group. Under cold stress, the expression of *Ascirbp* gene did not change significantly at 15°C ($P > 0.05$).

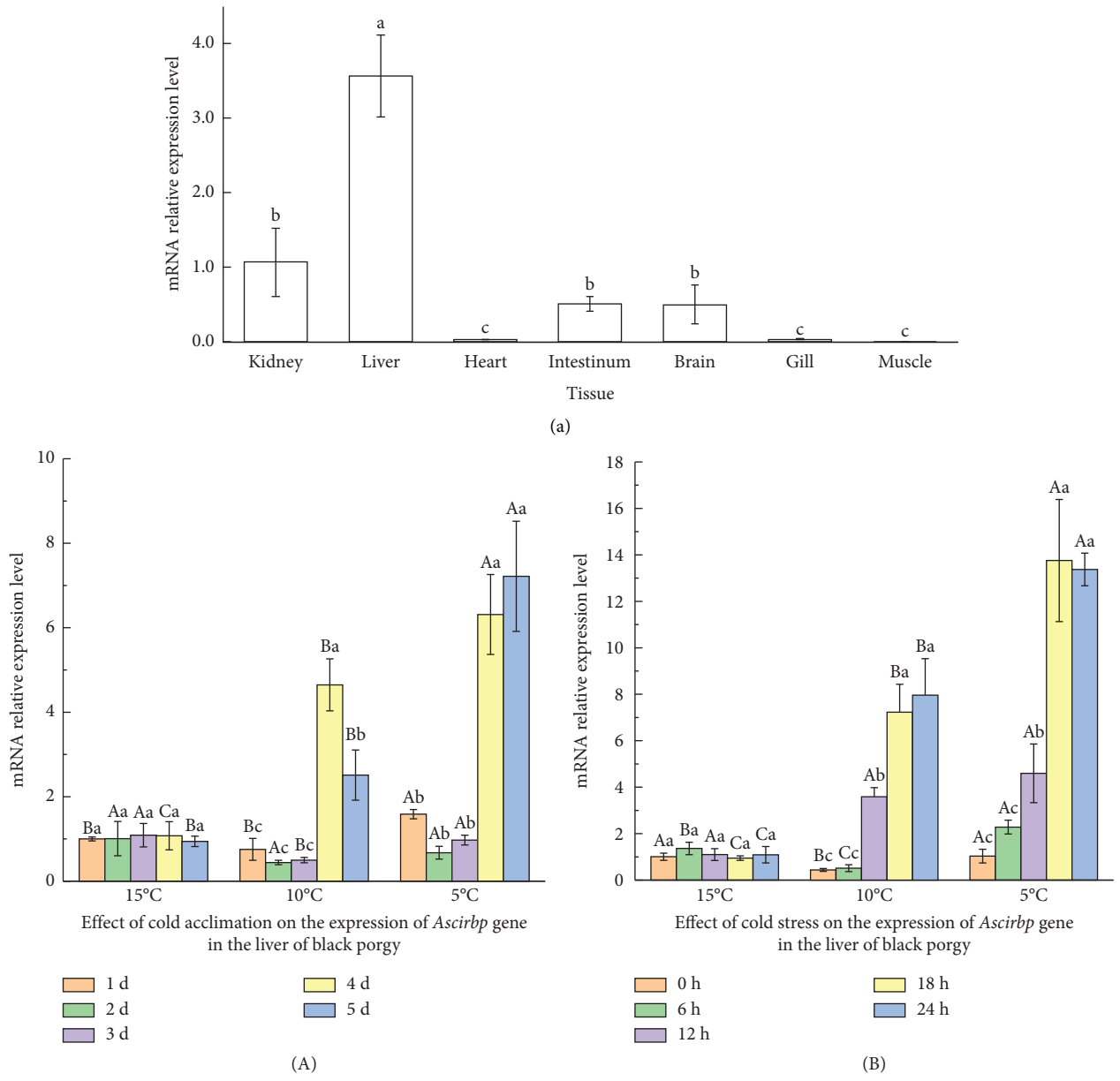

Figure 5: Continued.

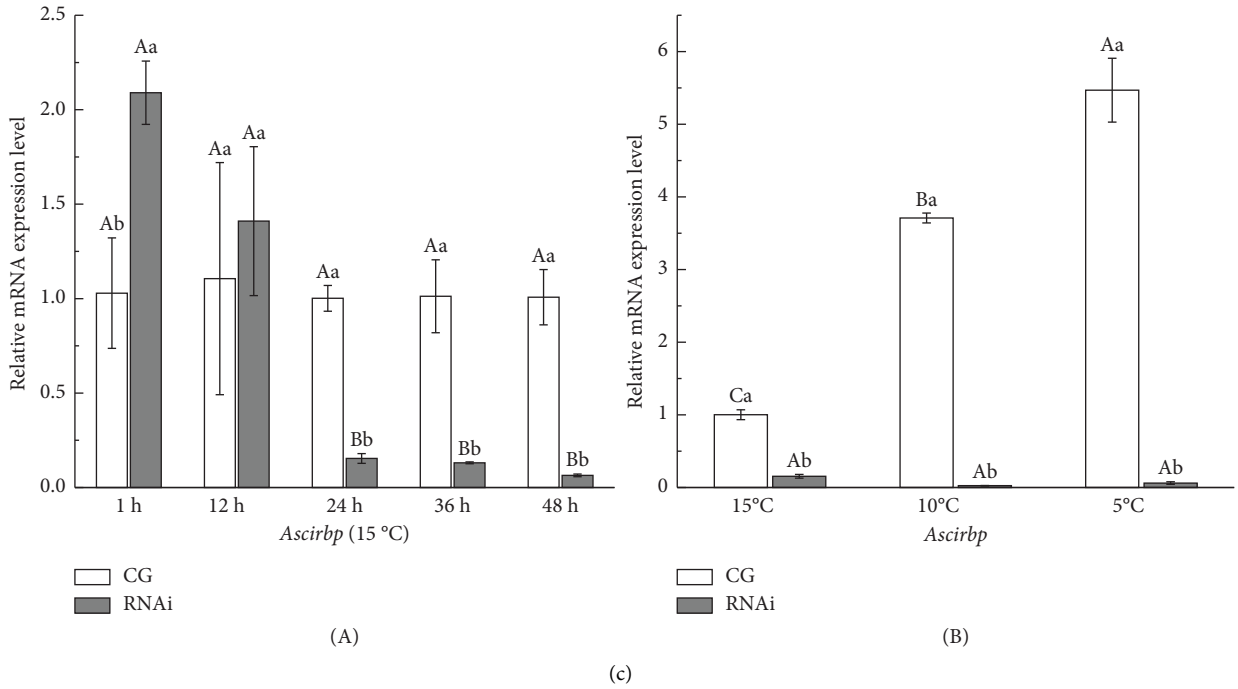

Figure 5: (a): Expression of *Ascirbp* gene in different tissues of the black porgy (15°C) ($n = 3$; X = mean ± SE); (b) effect of different cooling ways on the expression of *Ascirbp* gene in the liver of black porgy ($n = 3$; X = mean ± SE); (c) effect of *Ascirbp*-dsRNA injection on the expression of *Ascirbp* gene in the liver of black porgy at different temperatures. Different lowercase letters above the square bars indicate significant differences within groups ($P < 0.05$), and the same lowercase letters indicate no significant differences within groups ($P > 0.05$). Different uppercase letters indicate significant differences between groups ($P < 0.05$), and the same uppercase letter indicates no significant difference between groups ($P > 0.05$).

At 10°C, the expression of *Ascirbp* gene was significantly lower than that of the control group at 0 h and 6 h ($P < 0.05$), and significantly higher after 12 h ($P < 0.05$). The expression of *Ascirbp* gene was also not significantly changed at 15°C under cold acclimation ($P > 0.05$). At 10°C, the expression of *Ascirbp* gene was significantly lower than the control group at 3 d and significantly higher than the control group after 4 d ($P < 0.05$). At 5°C, the expression of *Ascirbp* gene was significantly higher than the control group after 1 d, 4 d, and 5 d ($P < 0.05$).

3.5. Effects of RNAi on the Relative Expression Level of Ascirbp Gene. At normal water temperature (15°C), the expression level of *Ascirbp* gene in the RNAi group (Figures 5(a)–5(c)) was significantly higher than in the control group at 1 h ($P < 0.05$), and did not have significant difference with the control group at 12 h ($P > 0.05$). At 24 h, 36 h, and 48 h after injection, the expression of *Ascirbp* gene in the RNAi group was significantly lower than that in the control group ($P < 0.05$), while the control group had no significant change during the whole RNAi experiment ($P > 0.05$). At 15°C, 10°C, and 5°C (Figures 5(b) and 5(c)), the expression of the control group showed an increase with decreasing temperature after keeping for 24 h. The expression of the RNAi group was significantly lower than that of the control group ($P > 0.05$) and there was no significant change with decreasing temperature ($P < 0.05$).

3.6. Effects of RNAi on the Tissue Structure of Liver in Black Porgy. At 15°C (Figure 6), the shape of the hepatocytes in the control group (CG) and RNAi group was oval or quadrilateral, with obvious connections between cells; the nuclei were round and located in the center or edge. At 10°C (Figure 6), the nuclei of hepatocytes in the CG were located on the intracellular side and showed pyknosis. Conspicuous hepatic structural abnormalities, derangement of the hepatic plate, and tissue vacuolation were found in the RNAi group. At this point, the nuclei of the hepatocytes disappeared and a large number of inflammatory cells appeared in the liver of the black porgy. At 5°C (Figure 6), hepatocytes of black porgy in the CG were irregularly geometrical, some nuclei disappeared or showed contraction, the cell structure was broken, and the vacuolation phenomenon was aggravated. Compared to the CG, a large number of hepatocytes in the RNAi group had broken structures and disappeared nuclei. The liver was also accompanied by a large number of vacuoles and inflammatory vesicles at this time.

3.7. Effects of RNAi on the Apoptosis of Liver in Black Porgy. After TUNEL staining, apoptotic cells in the liver appear brown (Figure 7(a)). At 15°C, there were no apoptotic cells in the liver sections of the control group, and apoptosis was already present in the RNAi group. At 10°C, the apoptotic cells in the control group started to appear sporadically. The number of apoptotic cells in the RNAi group gradually

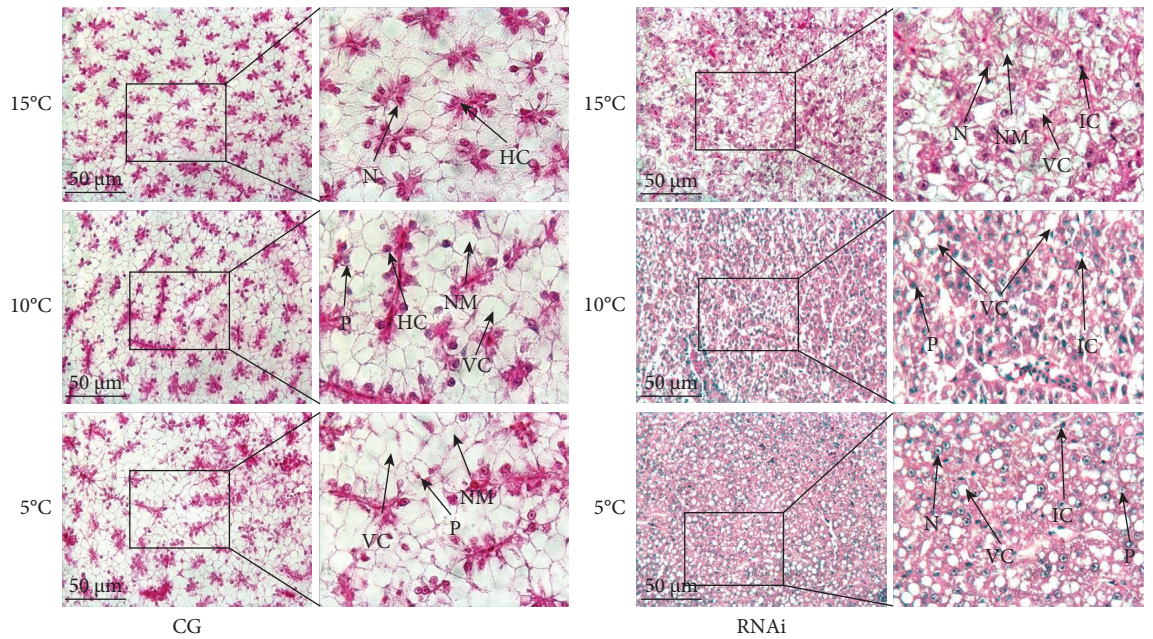

Figure 6: Effect of *Ascirbp*-dsRNA injection on liver tissue structure of the black porgy ($n = 3$). CG. control group; RNAi. RNA interference group; HC. hepatocytes; VC. cavitation; N. nucleus; NM. nucleus missing; IC. inflammatory cell; P. pyknosis.

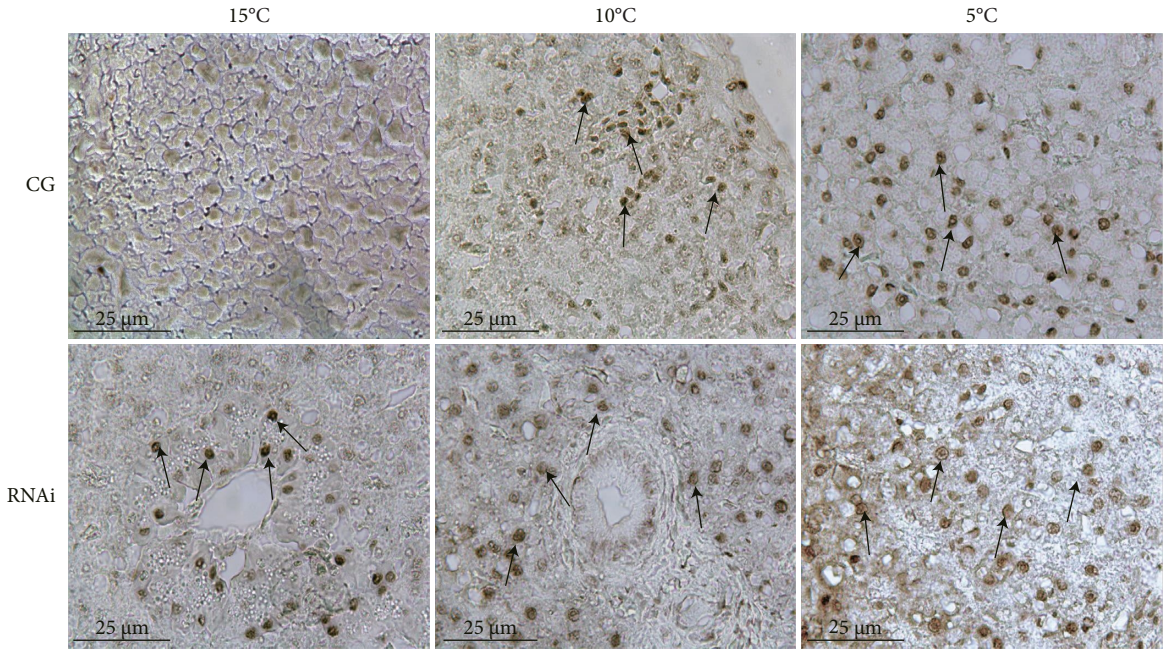

(a)

Figure 7: Continued.

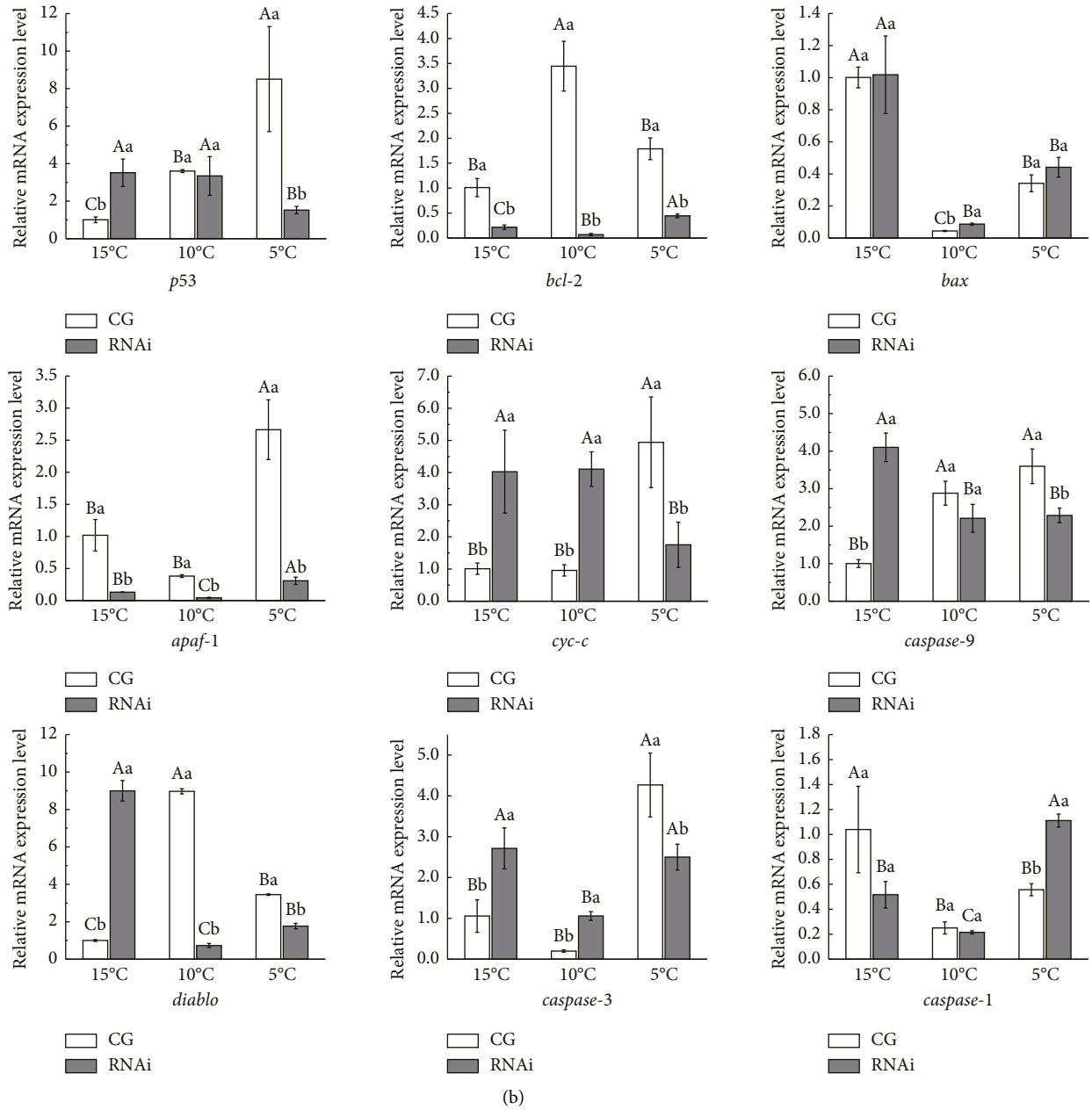

Figure 7: (a): Light microscopic observation (1000×) of apoptosis in the liver of black porgy in the control group (CG) and RNA interference group (RNAi) at different temperatures by using TUNEL staining method ($n = 3$); the black arrows in the diagram refer to apoptotic cells. (b) Expression of apoptosis genes in the liver of black porgy after silencing the expression of *Ascirbp* gene ($n = 3$; X = mean ± SE). Note: different lowercase letters above the square bars indicate significant differences within groups ($P < 0.05$), and the same lowercase letters indicate no significant differences within groups ($P > 0.05$); different uppercase letters indicate significant differences between groups ($P < 0.05$), and the same uppercase letter indicates no significant differences between groups ($P > 0.05$).

increased, and the number of apoptotic cells was more than that in the control group. At 5°C, the apoptosis of the liver in the control group and the RNAi group was aggravated.

3.8. Effects of RNAi on Key Genes in the Apoptosis Pathway of the Liver in Black Porgy. After RNAi experiments on black porgy (Figure 7(b)), the expression of *p*53 gene in the RNAi group was significantly higher in the 15°C group than in the control group ($P < 0.05$) and lower in the 5°C group than that in the control group ($P < 0.05$). The expression of *bcl*-2 gene in the RNAi group was significantly lower than that in the control group at different temperatures and the expression was highest at 5°C ($P < 0.05$). The expression of *bax* gene in the RNAi group significantly higher than that in the control group at 10°C ($P < 0.05$). In the interfered group, the expression of *cyc-c* gene was significantly higher in both the 15°C and 10°C groups than in the control group, and lower

than in the control group at 5°C. The expression of *apaf*-1 gene in the RNAi group was significantly lower than in the control group at different temperatures ($P < 0.05$). In the interfered group, the expression of *caspase*-9 gene was significantly higher at 15°C than in the control group, and significantly higher at 10°C and 5°C than in the control group. The expression of *caspase*-3 gene in both groups decreased to the lowest level at 10°C. The expression of *caspase*-3 gene in the RNAi group was significantly higher than that in the control group at 15°C and 10°C ($P < 0.05$), and increased to the maximum level at 5°C and the expression was significantly higher than that in the RNAi group ($P < 0.05$). In the control group, the expression of *diablo* gene was significantly higher at 10°C and 5°C ($P < 0.05$) and reached the maximum at 10°C ($P < 0.05$). In the RNAi group, the expression of *diablo* gene was significantly higher at 15°C than in the control group and significantly lower at 10°C and 5°C ($P < 0.05$). The expression of *caspase*-1 gene in the RNAi group was significantly higher than that in the control group at 5°C ($P < 0.05$).

4. Discussion

4.1. Molecular Cloning and Tissue Expression Analysis of Ascirbp Gene in Black Porgy. CIRBP is first identified in mammals and is determined to be located in the nucleus by immunohistochemistry [15, 31]. In this study, the subcellular localization of AsCIRBP was predicted to be in the nucleus and these were consistent with the findings in mammals. CIRBP is a class of RNA-binding proteins with a highly conserved glycine-rich sequence with the RNA-binding region, the RNA recognition motif (RRM) [32]. Meanwhile, the RRM was also found in the ORF of *Ascirbp* gene. Under normal or pathological conditions, RRM of CIRBP can affect the stability of RNA molecules, splicing, nuclear export and translation of target gene transcription sequences. However, it can't affect the transcription level of target RNA [33]. For example, CIRBP can bind to mRNAs encoding adhesion molecules, T-cell factor-3 (TCF-3), and other genes, thereby regulating the development of embryos of *Xenopus laevis* [34].

The *cirbp* gene is widely distributed in various animal tissues. For example, it is expressed in the brain, liver, heart, and other tissues in humans and mice [35]. In this study, the mRNA transcripts of *Ascirbp* from black porgy were more abundant in the liver, where they were exceptionally high than other tissues. Previous studies have shown that the *cirbp* gene of *Takifugu obscurus* is most highly expressed in the liver, which consistent with the present results [20]. CIRBP as a cold stress protein, it shows a significant increase at low temperatures. In the liver of black porgy, the expression of *Ascirbp* gene was significantly increased at low temperature in both cold stress and cold acclimation. However, *Ascirbp* gene responded more rapidly to low temperature under cold stress than to cold acclimation. The result is similar to the expression pattern of *cirbp* gene in the liver of *Takifugu obscurus* [27], *Larimichthys crocea* [28] and *Paralichthys olivaceus* [36] at low temperatures. Therefore, we get a conclusion that response time of *Ascirbp* gene to environmental low temperature is different under different cooling patterns.

4.2. Functional Analysis of Ascirbp Gene in Black Porgy Based on RNAi Technique. According to recent reports, the researchers have successfully verified the function of the *slc7a11* gene in red tilapia to regulate the melanogenesis pathway through RNAi technique [30]. In this study, *Ascirbp* gene expression in the liver of black porgy was also successfully silenced by RNAi technique at different temperatures. The results of H.E staining showed that the hepatocytes of black porgy showed pyknosis, nucleus disappearance and cell vacuolation at 5°C in the control group, which is similar to the results of the histological changes in the liver of black porgy at low temperatures [5]. Compared to the control group, the livers of black porgy in the RNAi group showed a large number of inflammatory cells, gaps between hepatocytes and vacuoles after cooling. Some studies showed that myocardial injury and inflammation induced by high glucose (HG) were more severe when the expression of CIRBP was silenced [37, 38]. After silencing the expression of the *Ascirbp* gene, the liver of black porgy was also more susceptible to inflammatory cells, cytolysis, cell membrane damage, and vacuolization at low temperature. In zebrafish with acute kidney injury, many inflammatory factors led to pyroptosis after kidney cell damage occurs [39]. Initial observations suggest that there may be a linkage between *Ascirbp* gene and pyroptosis. Pyroptosis is a programmed process of cell death. The process is a continuous expansion of cells until the cell membrane ruptures, which leads to the release of cellular contents and activates a strong inflammatory response [40]. In this mechanism, the classical pathway of pyroptosis activates Caspase-1 protein, which cleaves and activates the inflammatory factors that stimulate pyroptosis [41]. When the cell membrane is damaged, CIRBP becomes an inflammatory factor and induces an inflammatory response [42]. However, those findings cannot be extrapolated to all cases. Recent research has suggested that CIRBP could act as a protective factor [37]. In ischemia-reperfusion injury of nerve cells, CIRBP activates the Akt and ERK signaling pathways, thus protecting nerve cells against oxidative stress [31]. At 5°C, hepatocytes of black porgy in the RNA interference group showed characteristics of pyroptosis and a significant increase expression in *caspase*-1 gene. Meanwhile, the results of the control group were the opposite. A probable explanation is that the *Ascirbp* gene can be a protective factor to reduce the inflammatory response of hepatocytes and inhibit pyroptosis at low temperatures.

By TUNEL staining, the number of apoptotic hepatocytes in the control group gradually increased with decreasing temperature. These results prove these findings of the speculation that black porgy will induce apoptosis under stimulation of low temperature [5]. Some evidence suggests that cardiomyocytes of mice with heart failure are more prone to apoptosis after silencing the expression of the *cirbp* gene [43]. It is encouraging to compare those results with that hepatocytes in black porgy were more susceptible to

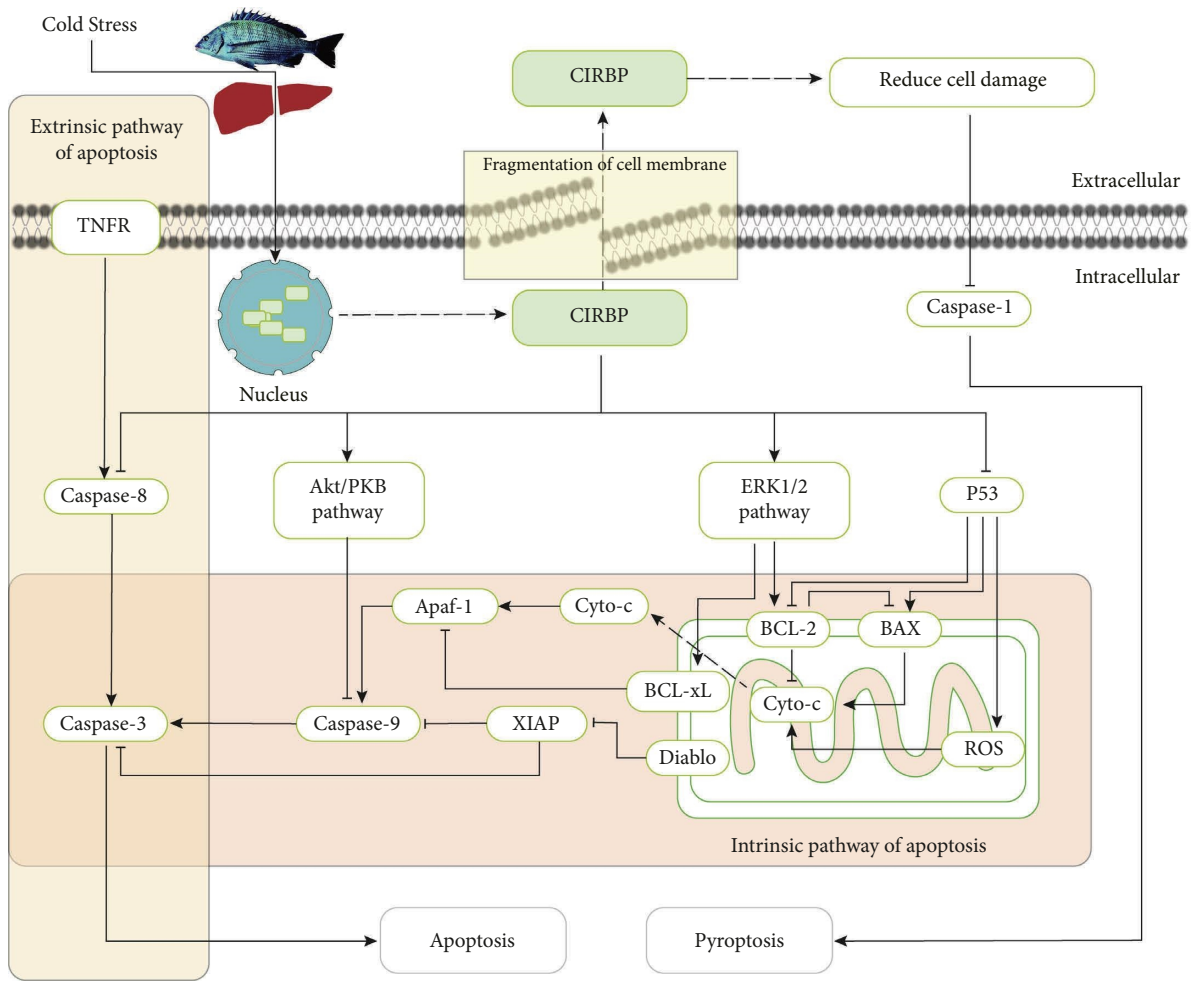

FIGURE 8: A proposed model for the molecular mechanisms of acute cold stress in the liver of black porgy. Arrows express promotion, dashed arrows indicate transfer, and T-bar represents inhibition.

apoptosis at low temperatures after silencing the expression of the *Ascirbp* gene.

The results of TUNEL staining reported here appear to support the assumption that the *Ascirbp* gene has the function of inhibiting apoptosis in the liver of black porgy. In recent years, many studies have found that CIRBP can inhibit apoptosis [13, 19]. CIRBP can delay apoptosis in skeletal muscle cells of mouse through the AKT signaling pathway under acute hypothermia [13]. Therefore, it seems to be a definite need for examining the expression changes of key genes of apoptosis to further understand the association between CIRBP and apoptosis in the liver of black porgy. It has been claimed that the *cirbp* gene is able to inhibit the expression of *p*53 gene [20, 44]. However, expressions of the *Ascirbp* gene and *p*53 gene in the liver of the control black porgy showed a significantly increase at low temperatures. When the expression of the *Ascirbp* gene was inhibited, the expression of *p*53 gene was significantly higher in the RNAi group at 15°C than in the control group. One research finds that CIRBP inhibits etoposide-induced apoptosis by regulating the expression levels of *p53* [44]. So, the result of this study suggests that the *Ascirbp* gene in the liver is able to suppress the expression of *p*53 gene at normal temperature. But the suppression of *p*53 gene by *Ascirbp* gene decreases gradually when the temperature decreases. In addition to this, *cirbp* gene can mediate the mitochondrial apoptotic pathway by regulating *bcl*-2 gene and *bax* gene [45]. The researchers have also found that reduced expression of antiapoptotic proteins (Bcl-2 and Bcl-xL proteins) in mice knocked out the CIRBP protein [46]. In this study, *bcl*-2 gene expression was also significantly inhibited after silencing the expression of *Ascirbp* gene. Bcl-2 protein can release cytochrome c (*cyto-c*) into the cell by regulating the permeability of the mitochondrial membrane at the beginning of apoptosis [47]. Bax protein can allow some ions and small molecules such as Cyto-*c* to pass through the mitochondrial membrane and enter the cytoplasm [48]. In this study, the expression of *bax* gene in the RNAi group was significantly higher than control group at 10°C. One possible implication is that inhibits the expression of Bcl-2 protein or promote the expression of Bax protein can result in mitochondria releases large amounts of Cyto-c into the cytoplasm [47, 48]. In RNAi group, the expression of *cyto*-c gene was significantly increased at 15°C and 10°C after silencing the expression of *Ascirbp* gene. This result suggests that *Ascirbp* gene can inhibit the expression of Cyto-c gene through

promoting expressions of *Ascirbp* gene and *bcl*-2 gene. Under normal circumstances, Cyto-c can activate the Apaf-1 protein to bind to the Caspase-9 protein to form an apoptotic protein and induce endogenous apoptosis of Caspase-3 protein [49]. In this study, *apaf*-1 gene expression was significantly inhibited after silencing the expression of *Ascirbp* gene. The result interdicts the pathway between *cyto*-c gene and *caspase*-9 gene, and leads to decrease in the expression of *caspase*-9 gene. The low-expression level of Apaf-1 protein makes Apaf-1 protein to be a limiting factor in the formation of apoptosome and the signaling of apoptosis [50]. The low expression of *caspase*-9 gene in the RNAi group confirmed this view. Previous study shows that the expression of *caspase*-9 gene, the apoptotic index and the apoptosis rate are significantly reduced after silencing the expression of the *apaf*-1 gene in PC12 cells [51]. Cells in Apaf-1 knockout mice can inhibit apoptotic under the stimulation of external environment [52]. It is speculated that the inhibition of *apaf*-1 gene expression in the RNAi group is due to regulation of *bcl-xL* gene. Bcl-xL protein is an important member of Bcl-2 protein family [53]. Bcl-XL protein not only inhibits the release of *cyto-c*, but also binds to Apaf-1 and Caspase-9 to form a ternary complex [54, 55]. The complex can block the cascade reaction and exert an inhibitory effect on apoptosis [54, 55]. Unfortunately, the function of *bcl-xL* gene was not explored in our study. The role of this gene in black porgy needs to be further explored. In addition to apoptosis induced by Cyto-c, Diablo protein can also induce apoptosis. Diablo protein on the mitochondrial membrane can bind to the interlocking inhibitor of apoptosis protein family (XIAP) to enhance apoptotic signaling and promote Caspase-9 and Caspase-3 proteins [51, 56]. In the mitochondrial apoptotic pathway, Caspase-3 protein is activated by Caspase-9 protein to perform apoptosis [56]. Compared with the control group, the liver of black porgy in the RNAi group appeared apoptosis at 15°C. This result may be explained by the fact that black porgy increases expression of *diablo* gene to promote expressions of *caspase*-9 gene and *caspase*-3 gene. Ultimately, it led to apoptosis in the liver of black porgy at normal temperatures. These findings from the study suggest that *Ascirbp* gene can have an effect on apoptosis. A proposed role of CIRBP in acute cold stress in the liver is demonstrated in Figure 8.

5. Conclusion

The research found the existence of apoptosis in black porgy liver at low temperatures and verified the function of *Ascirbp* gene in inhibiting apoptosis of hepatocytes at cold stress. These results provide strong theoretical support for subsequent experiments such as editing and overexpression of *Ascirbp* gene in the black porgy. Based on these results, it is more helpful for us to create low temperature resistant species of black porgy.

Data Availability

The data that support the findings of this study are all generated by the experiments. The sequence of *Ascirbp* gene has been uploaded to National Center for Biotechnology Information (NCBI). The Gene ID is ON063224 https://www.ncbi.nlm.nih.gov/nuccore/ON063224.2/.

Conflicts of Interest

The authors declare that there are no conflicts of interest.

Authors' Contributions

Mingliang Wei, Zhiwei Zhang, Zhiyong Zhang, Mingjun Shen, and Yue Wang design the experiment. Mingliang Wei, Mingjun Shen, Yue Wang, Bo Gao, Ruijian Sun, Yali Qin, Jing Shen, Xiaojian Tang, Jianbin Jiang, and Jianlou Zhou did the experiment; Mingliang Wei, Zhiwei Zhang, and Mingjun Shen wrote the paper.

Acknowledgments

This work was financially supported by the Key Project for Natural Science Foundation of Jiangsu Province "Investigating the mechanism of low-temperature tolerance and its molecular mechanism in black porgy based on multiomics technology" (grant/award number: BK20221268); Jiangsu Agricultural New Variety Innovation "Genetic improvement of seabream and creation of new strains" (grant/award number: PZCZ201744); Jiangsu Provincial "333 Project" Talent Funding "Exploring the low temperature tolerance mechanism and genetic mechanism of black porgy based on whole genome and transcriptome data" (grant/award number: BRA2020372); and Jiangsu Provincial Agricultural Project "Conservation and renewal of improved aquatic species" (grant/award number: 2022-SJ-009). Major Agricultural Technology Collaborative Promotion Project, "Green and healthy culture technology of marine economic fish" (grant/award number: 2021-ZYXT-09).

References

[1] Z. Zhang, Z. Lin, M. Wei et al., "Development of single nucleotide polymorphism and association analysis with growth traits for black porgy (Acanthopagrus schlegelii)," *Genes*, vol. 13, no. 11, 2022.

[2] J. Qiang, Z. Zhang, J. Yu et al., "Water quality and physiological response of F1 hybrid seabream (Pagrus major schlegelii stress at different densities)," *Aquaculture Research*, vol. 49, no. 2, pp. 767–775, 2017.

[3] Z. Lin, Z. Zhang, F. Solberg et al., "Comparative transcriptome analysis of mixed tissues of black porgy (Acanthopagrus schlegelii) with differing growth rates," *Aquaculture Research*, vol. 55, no. 11, pp. 5800–5813, 2021.

[4] X. Li, Y. Shen, Y. Bao et al., "Physiological responses and adaptive strategies to acute low-salinity environmental stress of the euryhaline marine fish black seabream (Acanthopagrus schlegelii)[J]," *Aquaculture*, vol. 55, no. 738117, 2022.

[5] M. Wei, Z. Zhang, Z. Zhang et al., "Effects of cold stress on black porgy (Acanthopagrus schlegelii) tissue injury and apoptosis gene expression," *South China Fisheries Science*, vol. 18, no. 05, pp. 110–117, 2022.

[6] J. Sun and J. Hong, "Effect of overwintering on body composition, antioxidant enzyme activities, fatty acid composition, glucose and lipid-metabolic related gene expression of

grass carp (Ctenopharyngodon idellus)," *Aquaculture*, vol. 545, no. 737125, 2021.

[7] Y. Awasthi, A. Ratn, R. Prasad, M. Kumar, and P. Trivedi, "An in vivo analysis of Cr^{6+} induced biochemical, genotoxicological and transcriptional profiling of genes related to oxidative stress, DNA damage and apoptosis in liver of fish, Channa punctatus (Bloch, 1793)," *Aquatic Toxicology*, vol. 200, pp. 158–167, 2018.

[8] D. Bertheloot and S. Franklin, "Necroptosis, pyroptosis and apoptosis: an intricate game of cell death," *Cellular and Molecular Immunology*, vol. 18, pp. 1106–1121, 2021.

[9] J. Luan and P. Xu, *Review on Programmed Cell Death and Vertebrate Embryonic Development*, Zhejiang University (Agriculture and Life Sciences), Hangzhou, China, 2023.

[10] M. Malumbres and M. Barbacid, "Cell cycle, CDKs and cancer: a changing paradigm," *Nature Reviews Cancer*, vol. 9, no. 3, pp. 153–166, 2009.

[11] A. Lujan and S. Hartley, "Cold-inducible RNA binding protein in cancer and inflammation," *Wiley Interdisciplinary Reviews _ RNA*, vol. 9, no. 2, p. e1462, 2018.

[12] Y. Liao, L. Tong, L. Tang, and S. Wu, "The role of cold-inducible RNA binding protein in cell stress response," *International Journal of Cancer*, vol. 141, no. 11, pp. 2164–2173, 2017a.

[13] Y. Liu, P. Liu, Y. Hu et al., "Cold-induced RNA-binding protein promotes glucose metabolism and reduces apoptosis by increasing AKT phosphorylation in mouse skeletal muscle under acute cold exposure," *Frontiers in Molecular Biosciences*, vol. 8, Article ID 685993, 2021.

[14] K. Saito, N. Fukuda, T. Matsumoto et al., "Moderate low temperature preserves the stemness of neural stem cells and suppresses apoptosis of the cells via activation of the cold inducible RNA binding protein," *Brain Research*, vol. 1358, pp. 20–29, 2010.

[15] E. Lleonart, "A new generation of proto-oncogenes: cold-inducible RNA binding proteins," *Biochimica et Biophysica Acta (BBA) Reviews on Cancer*, vol. 1805, no. 1, pp. 43–52, 2010.

[16] C. Gueydan, V. Kruys, G. Huez, C. Wauquier, T. Zhang, and D. Leeuw, "The cold-inducible RNA-binding protein migrates from the nucleus to cytoplasmic stress granules by a methylation-dependent mechanism and acts as a translational repressor," *Experimental Cell Research*, vol. 313, no. 20, p. 4130, 2007.

[17] H. Zhang, J. Xue, Z. Zhang et al., "Cold-inducible RNA-binding protein inhibits neuron apoptosis through the suppression of mitochondrial apoptosis," *Brain Research*, vol. 1622, pp. 474–483, 2015.

[18] S. Kesavardhana, S. Malireddi, and T. Kanneganti, "Caspases in cell death, inflammation, and gasdermin-Induced pyroptosis," *Annual Review of Immunology*, vol. 38, no. 1, pp. 567–595, 2020.

[19] L. Wu, H. Sun, Y. Gao et al., "Therapeutic hypothermia enhances cold-inducible RNA-binding protein expression and inhibits mitochondrial apoptosis in a rat model of cardiac arrest," *Molecular Neurobiology*, vol. 54, pp. 2697–2705, 2016.

[20] H. Gao, R. Xie, R. Huang et al., "CIRBP regulates pancreatic cancer cell ferroptosis and growth by directly binding to p53," *Journal of Immunology Research*, vol. 2022, Article ID 2527210, 12 pages, 2022a.

[21] U. Mushtaq, J. Åden, A. Clifton, T. Sparrman, and G. Grobner, "Unravelling the molecular basis of cell protection by BCL-2 proteins," *Biophysical Journal*, vol. 121, no. 3, p. 169, 2022.

[22] L. Bai, J. Yang, H. Zhang, W. Liao, and Y. Cen, "PTB domain and leucine zipper motif 1 (APPL1) inhibits myocardial ischemia/hypoxia-reperfusion injury via inactivation of apoptotic protease activating factor-1 (APAF-1)/Caspase9 signaling pathway," *Bioengineered*, vol. 12, no. 1, pp. 4385–4396, 2021.

[23] M. Srinivasula, P. Datta, X. Fan, T. Fernandes-Alnemri, Z. Huang, and S. Alnemri, "Molecular determinants of the caspase-promoting activity of smac/DIABLO and its role in the death receptor pathway," *Journal of Biological Chemistry*, vol. 275, no. 46, pp. 36152–36157, 2000.

[24] C. Ribeiro and G. Szabo, "Role of the inflammasome in liver disease," *Annual Review of Pathology: Mechanisms of Disease*, vol. 17, no. 1, pp. 345–365, 2021.

[25] J. Hu, F. You, Q. Wang, L. Wang, S. Weng, and M. Xin, "Cloning and expression analysis of cold-tolerance related genes, CIRP and HMGB1, in Paralichthys olivaceus," *Marine Sciences*, vol. 39, no. 01, pp. 29–38, 2015.

[26] L. Tian, Q. You, C. Chi, H. Song, and D. Xu, "Characterization of cold-tolerance related genes,CIRP and nefm in Nibea albiflora by cloni and expression analysis," *Journal of Zhejiang Ocean University*, vol. 38, no. 4, pp. 286–294+308, 2019.

[27] Y. Gao, C. Wang, X. Liu, X. Liang, Z. Zhao, and Y. Shi, "Molecular characterization of cold-tolerance related genes CIRBP, HMGB1, AFP-IV from Takifugu obscurus and their response to low temperature stress," *Acta Hydrobiologica Sinica, Online*, vol. 34, pp. 1–12, 2022b.

[28] L. Miao, M. Li, Y. Chen, M. Hu, and J. Chen, "Cloning of cold inducible RNA-binding protein (CIRP) gene in Larimichthys crocea and its expression analysis under cold treatments," *Journal of Fisheries of China*, vol. 41, no. 4, pp. 481–489, 2017.

[29] Z. Zhang, K. Zhang, S. Chen et al., "Draft genome of the protandrous Chinese black porgy," *Acanthopagrus schlegelii, GigaScience*, vol. 7, no. 4, pp. 1–7, 2018.

[30] L. Wang, H. Bu, F. Song, W. Zhu, J. Fu, and Z. Dong, "Characterization and functional analysis of slc7a11 gene, involved in skin color differentiation in the red tilapia," *Comparative Biochemistry and Physiology A Part A Molecular & Integrative Physiology*, vol. 236, Article ID 110529, 2019.

[31] J. Liu, J. Xue, H. Zhang et al., "Cloning, expression, and purification of cold inducible RNA-binding protein and its neuroprotective mechanism of action," *Brain Research*, vol. 1597, pp. 189–195, 2015.

[32] O. Ciuzan, J. Hancock, D. Pamfil, L. Wilson, and M. Ladomery, "The evolutionarily conserved multifunctional glycine-rich RNA-binding proteins play key roles in development and stress adaptation," *Physiologia Plantarum*, vol. 153, no. 1, pp. 1–11, 2014.

[33] C. Burd and G. Dreyfuss, "Conserved structures and diversity of functions of RNA-binding proteins," *Science*, vol. 265, no. 5172, pp. 615–621, 1994.

[34] T. Uochi and M. Asashima, "XCIRP (Xenopus homolog of cold-inducible RNA-binding protein) is expressed transiently in developing pronephros and neural tissue," *Gene*, vol. 211, no. 2, pp. 245–250, 1998.

[35] Y. Liao, J. Feng, Y. Zhang, L. Tang, and W. Shiyong, "The mechanism of CIRP in inhibition of keratinocytes growth arrest and apoptosis following low dose UVB radiation," *Molecular Carcinogenesis*, vol. 56, no. 6, pp. 1554–1569, 2017b.

[36] X. Yang, J. Gao, L. Ma et al., "Molecular cloning, expression pattern, and 3D structural prediction of the cold inducible RNA-binding protein (CIRP) in Japanese flounder (Paralichthys olivaceus)," *Journal of Ocean University of China*, vol. 14, no. 1, pp. 161–170, 2015.

[37] H. Zhao, B. Wu, Y. Luo et al., "Exogenous hydrogen sulfide ameliorates high glucose-induced myocardial injury & inflammation via the CIRP-MAPK signaling pathway in H9c2 cardiac cells," *Life Sciences*, vol. 208, pp. 315–324, 2018.

[38] X. Zheng, Y. Fan, J. Li et al., "Change in oxidative stress and mitochondrial dynamics in response to elevated Cold-Inducible RNA-Binding protein in cardiac surgery-associated acute kidney injury," *Oxidative Medicine and Cellular Longevity*, vol. 2022, Article ID 3576892, 13 pages, 2022.

[39] T. Bergsbaken, L. Fink, and T. Cookson, "Pyroptosis: host cell death and inflammation," *Nature Reviews Microbiology*, vol. 7, no. 2, pp. 99–109, 2009.

[40] A. Mamun, A. Mimi, Y. Wu et al., "Pyroptosis in diabetes nephropathy," *Clinica Chimica Acta*, vol. 523, pp. 131–143, 2021.

[41] D. Molla, B. Ayelign, G. Dessie, Z. Geto, and D. Admasu, "Caspase-1 as a regulatory molecule of lipid metabolism," *Lipids in Health and Disease*, vol. 19, no. 1, 2020.

[42] M. Aziz and P. Wang, "Extracellular CIRP (eCIRP) and inflammation," *Journal of Leukocyte Biology*, vol. 106, no. 1, pp. 133–146, 2019.

[43] M. Chen, H. Fu, J. Zhang, H. Huang, and P. Zhong, "CIRP downregulation renders cardiac cells prone to apoptosis in heart failure," *Biochemical and Biophysical Research Communications*, vol. 517, no. 4, pp. 545–550, 2019.

[44] N. Lee, S. Ahn, and H. Jang, "Cold-inducible RNA-binding protein, CIRP, inhibits DNA damage-induced apoptosis by regulating p53," *Biochemical and Biophysical Research Communications*, vol. 464, no. 3, pp. 916–921, 2015.

[45] F. Su, S. Yang, H. Wang, Z. Qiao, and Q. Zhengyi, "CIRBP ameliorates neuronal amyloid toxicity via antioxidative and antiapoptotic pathways in primary cortical neurons," *Oxidative Medicine and Cellular Longevity*, vol. 2020, Article ID 2786139, 9 pages, 2020.

[46] S. Thangarajan, A. Vedagiri, S. Somasundaram, R. Sakthimanogaran, and M. Murugesan, "Neuroprotective effect of morin on lead acetate- induced apoptosis by preventing cytochrome c translocation via regulation of Bax/Bcl-2 ratio," *Neurotoxicology and Teratology*, vol. 66, pp. 35–45, 2018.

[47] B. Eid and N. El-Shitany, "Captopril downregulates expression of Bax/cytochrome C/caspase-3 apoptotic pathway, reduces inflammation, and oxidative stress in cisplatin-induced acute hepatic injury," *Biomedicine & Pharmacotherapy*, vol. 139, Article ID 111670, 2021.

[48] H. Wang, J. Zhu, L. Jiang et al., "Mechanism of Heshouwuyin inhibiting the Cyt c/Apaf-1/Caspase-9/Caspase-3 pathway in spermatogenic cell apoptosis," *BMC Complementary Medicine and Therapies*, vol. 20, no. 1, 2020.

[49] Z. Li, D. Guo, X. Yin et al., "Zinc oxide nanoparticles induce human multiple myeloma cell death via reactive oxygen species and Cyt-C/Apaf-1/Caspase-9/Caspase-3 signaling pathway in vitro," *Biomedicine & Pharmacotherapy*, vol. 122, Article ID 109712, 2020.

[50] H. Yoshida, Y. Kong, R. Yoshida et al., "Apaf1 is required for mitochondrial pathways of apoptosis and brain development," *Cell*, vol. 94, no. 6, pp. 739–750, 1998.

[51] J. Zhang, W. Gao, X. Zhou, and X. Jin, "Silence Apaf 1 gene for oxygen deprivation or after oxygen and after sugar PC12 cell mitochondrial apoptosis pathway," *Chinese Journal of Immunology*, no. 1, pp. 21–30, 2021.

[52] F. Cecconi, G. Alvarez-Bolado, I. Meyer, A. Roth, and P. Gruss, "Apaf1 (CED-4 Homolog) regulates programmed cell death in mammalian development," *Cell*, vol. 94, no. 6, pp. 727–737, 1998.

[53] S. Fujimura, J. Suzumiya, Y. Yamada, and M. Kuroki, "Downregulation of Bcl-xL and activation of caspases during retinoic acid-induced apoptosis in an adult T-cell leukemia cell line," *The Hematology Journal*, vol. 4, no. 5, pp. 328–335, 2003.

[54] Y. Hu, A. Benedict, D. Wu, N. Inohara, and G. Núñez, "Bcl-XL interacts with Apaf-1 and inhibits Apaf-1-dependent caspase-9 activation," *Proceedings of the National Academy of Sciences*, vol. 95, no. 8, pp. 4386–4391, 1998.

[55] G. Pan, K. O'Rourke, and M. Dixit, "Caspase-9, bcl-XL, and apaf-1 form a ternary complex," *Journal of Biological Chemistry*, vol. 273, no. 10, pp. 5841–5845, 1998.

[56] F. Attaran-Bandarabadi, A. Abhari, H. Neishabouri, and J. Davoodi, "Integrity of XIAP is essential for effective activity recovery of apoptosome and its downstream caspases by Smac/Diablo," *International Journal of Biological Macromolecules*, vol. 101, pp. 283–289, 2017.